



# Effects of Deposition Parameters on the Electrochemical Behaviour of ZnO Thin Film

著者	Zheng A.L.T., Andou Y., Zawawi R.M.
journal or publication title	Journal of Advanced Chemical Sciences
volume	3
number	4
page range	521-524
year	2017
URL	<a href="http://hdl.handle.net/10228/00006587">http://hdl.handle.net/10228/00006587</a>



Share Your Innovations through JACS Directory

# Journal of Advanced Chemical Sciences

Visit Journal at <http://www.jacsdirectory.com/jacs>

## Effects of Deposition Parameters on the Electrochemical Behaviour of ZnO Thin Film

Alvin Lim Teik Zheng<sup>1</sup>, Yoshito Andou<sup>2</sup>, Ruzniza Mohd Zawawi<sup>1,\*</sup><sup>1</sup>Department of Chemistry, Faculty of Science, Universiti Putra Malaysia, 43400 Serdang, Selangor Darul Ehsan, Malaysia.<sup>2</sup>Graduate School of Life Science and System Engineering, Kyushu Institute of Technology, Fukuoka, Japan.

### ARTICLE DETAILS

#### Article history:

Received 20 December 2017

Accepted 29 December 2017

Available online 16 January 2018

#### Keywords:

ZnO  
Electrodeposition  
Cyclic Voltammetry

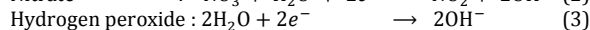
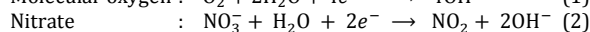
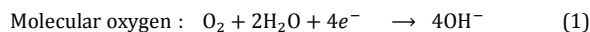
### ABSTRACT

In this work, the electrochemical deposition of zinc oxide (ZnO) thin film on indium tin oxide (ITO) glass substrate from aqueous zinc nitrate was studied. Among the deposition parameters employed were deposition temperature, deposition potential, and deposition time. The morphology of the ZnO thin film was studied via FESEM. The electrochemical behaviour of the deposited ZnO thin film was studied via cyclic voltammetry (CV) experiments. The deposition parameters lead to significant influence on the morphology and electrochemical behaviour of the thin films. The coverage area of the nanorods increased with the increase of temperature. Irregular structures of ZnO were obtained at lower deposition temperature at 60 °C. However, as the temperature increased to 90 °C, hexagonal shaped nanorods could be observed. As for the deposition potential, as the potential becomes more negative, more nucleation centers are activated and the rods are more vertical. The surface coverage is small, and increases with the deposition time. The compactness of the ZnO deposited is the highest with hexagonal rods covering the substrate at higher deposition time. The optimum electrochemical behavior of ZnO modified electrode was obtained from the deposition temperature of 60 °C using a deposition potential of -0.9 V for 900 seconds.

### 1. Introduction

Nanostructured electrodes encompass the idea of modifying the electrodes surface by organic monolayers modification of electrode surfaces or hybrid modification layers involving organic monolayers and nanomaterials [1]. These structures were incorporated in order to increase the electroactive surface area and electrochemical signals which is to achieve a high surface-to-volume ratio. The increase in the electroactive surface area allows for higher sensitivity and a lower detection limit [2]. However, the biggest predicament is the need of control over the distribution and size of the nanoparticles on the electrodes in obtaining a high surface area electrode. The commonly used method in incorporating nanostructures on the surface of the electrode is through electrodeposition which is a viable technique to control the amount of material to be deposited on the surface.

Zinc oxide (ZnO) nanostructure is an n-type semiconductor having transparent wide band gap (3.3 eV) with a large excitation binding energy (60 meV) has vast potential in various applications such as solar cells, sensors, and piezoelectric. There are various fabrication techniques of ZnO nanostructure such as precipitation [3], chemical vapour deposition [4], hydrothermal [5] and electrodeposition [6]. The cathodic electrodeposition is an emerging method preferred over other techniques due to its advantages such as low cost, low temperature processing and soft processing of materials [7]. The electrodeposition of ZnO is a flexible growth process in which an array of nanostructure could be obtained via this technique. The pioneers in this work were developed by Peulon and Lincot [8]. The reaction leading to the formation of ZnO was produced by hydroxide ions of an oxygen precursor such as oxygen, nitrate ions or hydrogen peroxide from the cathodic reduction. The general reaction for the production of hydroxide ion is supposed to follow the following equations:



The usage of ZnO modified electrode in sensor application is common due to its bio-compatibility, high catalytic efficiency and strong adsorption ability [9, 10]. Since the past years, various ZnO nanostructures such as nanorods [11], nanoparticles [12, 13] and nanowires [14] were reported to be used as a capable sensor with improved analytical performance. By controlling the preparation conditions such as temperature, deposition time and deposition potential during electrodeposition, a wide array of ZnO nanostructures can be obtained [15, 16]. The effect of temperature during deposition greatly affects the morphology and film thickness of the ZnO thin film. In the study conducted by Illy et al., [17] film was observed as small aggregated particles, and plate-like particles when electrodeposition was conducted at low temperature (below 60 °C). However at higher temperature rod like particles becomes more hexagonal in cross section of the film. It was found by them that more nucleation centers are activated with more vertical rods at lower deposition potential. The effect of deposition time has also shown to greatly affect the thickness of deposited film as well as the morphology of the film [18]. Hence, it is still a great challenge to obtain a simple fabrication process with the optimum deposition parameters with large active area and at the same time with good electrochemical capabilities that can be applied in sensor applications. Provided that there are a large number of reports on the electrodeposition of ZnO, the aim of this study is to study the optimum conditions using aqueous Zn(NO<sub>3</sub>)<sub>2</sub> bath.

### 2. Experimental Methods

#### 2.1 Materials

Conductive Indium-Tin Oxide (ITO) thin film electrodes with size (7 cm x 1 cm) were used as the glass substrate which was purchased from. Potassium ferricyanide (K<sub>3</sub>[Fe(CN)<sub>6</sub>]) were purchased from System Chemical, Zinc nitrate hexahydrate (Zn(NO<sub>3</sub>)<sub>2</sub>·6H<sub>2</sub>O) was purchased from Friendemann Schmidt. Potassium chloride (KCl), Ethanol (C<sub>2</sub>H<sub>5</sub>OH) and Acetone (CH<sub>3</sub>COCH<sub>3</sub>) were purchased from HmbG Chemicals while Hydrochloric acid (HCl, 37 %) from R&M Chemicals. All chemicals were of analytical grade and were used without further purification. All supporting electrolytes were prepared using ultrapure 18.2 M Ωcm deionized water obtained from Barnstead nanopure ultrapure water systems (Thermo Scientific).

\*Corresponding Author

Email Address: ruzniza@upm.edu.my (Ruzniza Mohd Zawawi)

## 2.2 Instrumentation and Electroanalytical Methods

The electrochemical measurement and electrochemical impedance spectroscopy (EIS) were carried out using an electrochemical analyzer Nova 1.1 Metrohm Autolab potentiostat (PGSTAT204, Metrohm Autolab, Netherlands) connected to an external computer. The electrochemical cell used consisted of a three electrode system setup. In general, this system is a potentiostatic circuit arranged in a manner that negligible current flows into the reference electrode which allows fairly accurate control of the potential across the working electrode thus granting a high degree of accuracy. A borosilicate electrolytic glass cell (20 mL) was used as the container to hold the electrolyte with a Teflon cap with holes for the placement of the electrodes and as an inlet and outlet for nitrogen gas. Due to this electrolysis process, the accurate determination of other species in the solution will be interfered. The purging of the inert nitrogen gas to remove the oxygen gas should be done for 1-2 minutes. The electrochemical cell used consisted of a three electrode system setup in which the electrodes used are indium tin oxide (ITO) as the working electrode, silver/silver chloride (Ag/AgCl) electrode with an internal solution of 3 M NaCl acting as a reference electrode and platinum wire as the counter electrode.

## 2.3 Fabrication of ZnO/ITO

Before any analysis was carried out, the ITO was cleaned with acetone, ethanol and distilled water respectively under ultrasonification for 15 minutes and subsequent drying in order to obtain a workable working electrode with a refurbished electrode surface. The purpose of these steps was to remove any thin layer coating of impurities at the ITO surface. Followed on was the rinsing and drying of the counter electrode and reference electrode using distilled water before being used. A 5 mL solution of 0.05 M zinc nitrate hexahydrate  $Zn(NO_3)_2 \cdot 6H_2O$  and 5 mL of 0.1 M of KCl were placed in the glass container and stirred for at least 10 minutes. Electrodeposition of ZnO was carried out using chronoamperometry (CA) technique using the electrochemical analyzer Nova 1.1 Metrohm Autolab potentiostat. Several parameters were employed in this procedure to electrodeposit the ZnO nanostructures, among them are varying temperature (60 °C to 90 °C), deposition time (900 s to 3600 s), and deposition potential (-0.9 V to -1.1 V). The modified electrode was then removed from the solution and rinsed with deionized water to remove any electrolyte residue from the glass substrate and dried under nitrogen gas stream for 10 minutes.

## 3. Results and Discussion

### 3.1 Electrochemical Studies

Cyclic voltammetry (CV) was performed to identify the presence of electrodeposition process and to study the electrochemical behaviour of the ZnO modified electrodes. Fig. 1 depicts the CV of the mixture containing 0.05 M  $Zn(NO_3)_2 \cdot 6H_2O$  and 0.1 M KCl solution onto the ITO glass substrate at 60 °C. Initially, the formation of zinc hydroxide,  $Zn(OH)_2$  takes place, followed at higher potentials by zinc oxide formation. From the voltammogram, the reduction of nitrate ions generates hydroxide ions occurring at around -0.68 V.

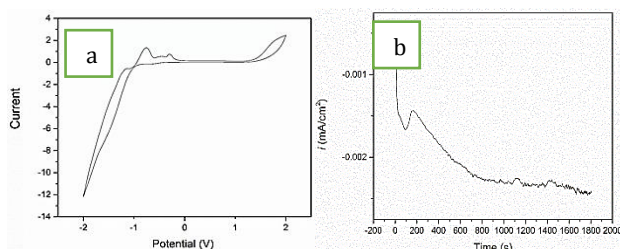
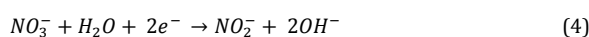


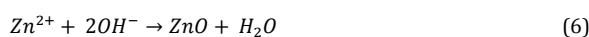
**Fig. 1** (a) Cyclic voltammogram of ITO substrate recorded in 0.05 M  $Zn(NO_3)_2 \cdot 6H_2O$  and 0.1 M of KCl solution at 60 °C with a scan rate of 100 mV/s (b) The current transient obtained in the electrodeposition of ZnO on ITO glass substrate using a deposition potential of -0.9 V in 60 °C bath solution at pH 7.0.



The following reaction reduces  $Zn^{2+}$  ions to metallic zinc,



occurring around -1.0 V.  $OH^-$  ions are produced which reacts with  $Zn^{2+}$  ions in the deposition solution forming ZnO:



The nucleation growth of ZnO onto ITO glass substrate was studied via the chronoamperometry (CA) technique. Fig. 1(b) depicts the current-time curves for the ZnO electrodeposition obtained at -0.9 V deposition potential for 1800 s. The process involved can be traced from the hike in current for a very short period of time followed by the current decay due to double layer discharging, and then the current rises due to the birth or nuclei on the surface and growth of the new phase. After the current reaches a maximum value, it decays again, until finally give a typical current – time profile at even longer times which is independent of the stepping potential [19]. This behavior can be attributed to the development of hemispherical diffusion zones around the growing nuclei which eventually overlap and coalesce corresponding to linear diffusion at a planar electrode [20]. If the rate of nucleation is rapid in comparison with the resultant rate of growth, subsequent nuclei are formed at all possible growth sites within very short times and nucleation is considered as instantaneous. However, if the rate of nucleation is slow, nucleation will continue to take place at the surface whilst previous nucleation centers continue to grow, and nucleation is termed progressive [21].

## 3.2 Morphology and Characterization of ZnO Thin Film

### 3.2.1 Effect of Temperature

Fig. 2 depicts the FESEM images of the ZnO coatings at various deposition temperature during electrodeposition. The growth temperature plays an important role on the hydroxylation and dehydroxylation reactions. When the deposition was carried out at <50 °C, rate of hydroxylation is faster than that of dehydroxylation [22]. Production of large amount of  $OH^-$  might suppress the faceted crystal growth by adsorbing on all possible crystal faces and this leads to the formation of crystallites. Irregular structures of ZnO are obtained at lower deposition temperature at 60 °C in this study. It can be seen that bundles of elongated and entangled nanowires surrounded by a large amount of tiny nanocrystals are deposited as depicted in Fig. 2(a). At 70 °C, aggregates of small grains are observed with uneven size could be seen deposited over a reasonably large area.

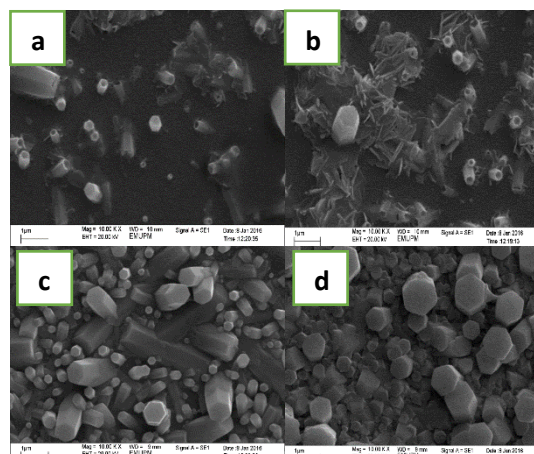
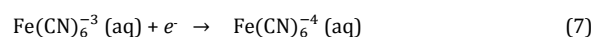


**Fig. 2** FESEM images of the ZnO nanorods (a) 60 °C (b) 70 °C (c) 80 °C (d) 90 °C at -0.9 V deposition potential for 1800 s

As the temperature is increased to 80 °C and 90 °C, the deposition of nanorods with a well-defined hexagonal trunk shape are seen to be deposited over the entire area which exhibits broad distribution. At 90 °C, the ZnO nanorods deposited are composed of separate rod-shaped grains with a well-defined cross hexagonal section which has different orientations and the film became more compact as depicted in Fig. 2(d).

The electrochemical characterization of the ZnO modified ITO electrode prepared at various deposition temperature ranging from 60 °C to 90 °C at a deposition potential of -0.9 V were carried out in the presence of  $K_3[Fe(CN)_6]$  in 0.1 M PBS electrolyte in order to evaluate the electrochemical behaviour. Ferricyanide ion undergoes a reversible one electron transfer [23]. The following reaction can be expressed as shown in Eq.(7).



From Fig. 3(a), it can be seen that the anodic peak current increased and the peak potential shifted to a more positive potential with the decrease in temperature. The voltammogram produced appears quasi reversible at the ZnO modified electrode prepared at 60 °C. The peak currents obtained are well defined with  $I_{pa}/I_{pc} = 1.059$  and a peak separation of 0.42 V. The

ZnO modified ITO prepared at 60 °C deposition temperature showed the best electrochemical response current of 251.83  $\mu\text{A}$  and -237.73  $\mu\text{A}$  at the anodic and cathodic peaks respectively. At 70 °C the redox peaks diminished to 142.79  $\mu\text{A}$  and -163.30  $\mu\text{A}$ . At 80 °C redox peaks continue to drop to 128.30  $\mu\text{A}$  and -124.02  $\mu\text{A}$ . While at 90 °C the redox peak current is at its lowest at 96.95  $\mu\text{A}$  and -107.64  $\mu\text{A}$  at the anodic and cathodic peaks respectively. The underlying reason behind the decrease of peak current with the increase of can be explained from the increase in film thickness as it increases with temperature. Based on Fig. 3(b), the ZnO modified electrode prepared at 60 °C increased by 2.60 fold for the oxidation peak when comparing to the ZnO modified electrode prepared at 90 °C.

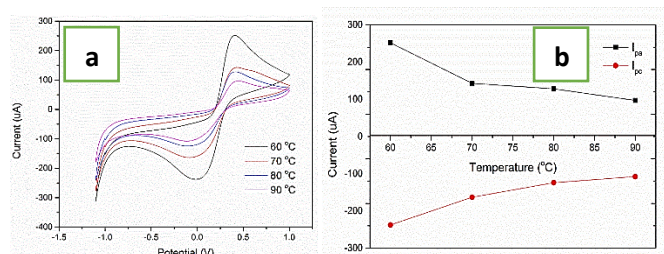


**Fig. 3** (a) Cyclic voltammogram of  $(\text{FeCN}_6)^{3-}$  at ZnO modified electrode prepared at 60 °C, 70 °C, 80 °C and 90 °C (b) Plot of anodic and cathodic peak currents obtained at various deposition temperature

### 3.2.2 Effect of Deposition Potential

Fig. 4 depicts the FESEM images of the ZnO thin film at various deposition potential during the electrodeposition process. The deposition potential also plays an important role on the hydroxylation and dehydroxylation reactions. It can be observed that the surface coverage of ZnO nanorods on the ITO glass spans a wide area. It can be seen that truncated ZnO are hexagonal in shape but not perpendicular to the substrate.

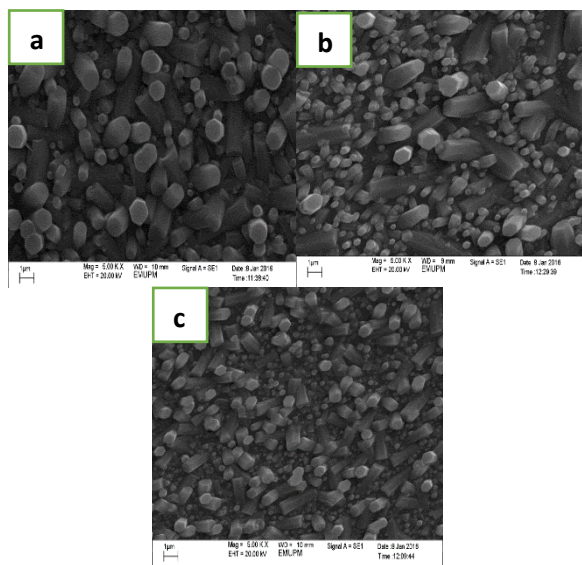


**Fig. 4** FESEM images of the ZnO nanorods (a) -0.9 V (b) -1.0 V and (c) -1.1 V at deposition temperature of 60 °C for 1800 s

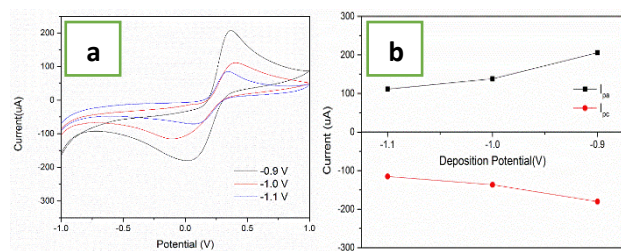


**Fig. 5** (a) Cyclic voltammogram of  $(\text{FeCN}_6)^{3-}$  at ZnO modified electrode deposited at -0.9 V, 1.0 V and -1.1 V at deposition temperature of 60 °C. (b) Plot of anodic and cathodic peak currents behavior of ZnO modified ITO obtained at various deposition potential

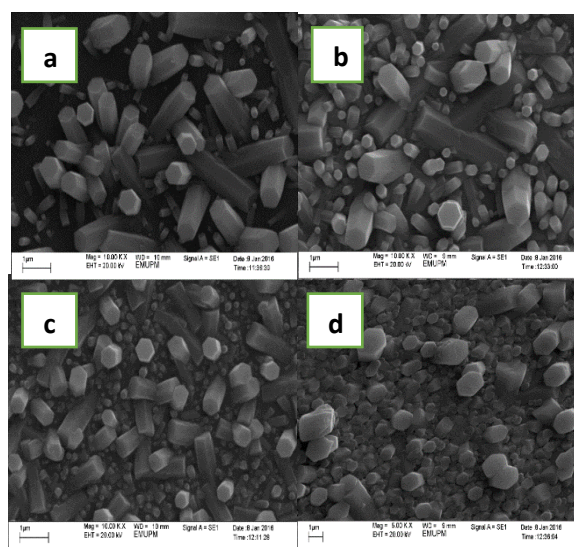
The higher the deposition potential, the less pore structures can only be observed at the bottom of plate crystals [24]. As the potential becomes more negative, more nucleation centers are activated and the rods are

more vertical. The low nucleation density occurs due to the molecular films have not been electrochemically activated and the electroreduction of oxygen and  $\text{NO}_3^-$  ions is kinetically slow [25].

Fig. 5(a) depicts the voltammogram of 1.0 mM  $\text{K}_3[\text{Fe}(\text{CN})_6]$  in 0.1 M PBS electrolyte solution at the ZnO modified ITO electrodes in the potential range of -1.0 V to 1.0 V. The cyclic voltammogram showed a well-defined redox couple for those three modified electrodes. The improvement in current signal enhancement for anodic and cathodic peak corresponds to the decrease of deposition potential from -1.1 V to -0.9 V. Based on Fig. 5(b), the ZnO modified ITO prepared at -0.9 V deposition potential showed the best electrochemical response current of 205.75  $\mu\text{A}$  and -180.18  $\mu\text{A}$  at the anodic and cathodic peaks respectively. The redox peaks diminished to 138.18  $\mu\text{A}$  and -136.72  $\mu\text{A}$  for -1.0 V deposition potential and 111.39  $\mu\text{A}$  and -115.05  $\mu\text{A}$  for -1.1 V deposition potential at the anodic and cathodic peaks respectively. As the negativity increases, the area of coverage of ZnO on the ITO glass substrate decrease and vice versa. By increasing the deposition potential, nanorods will grow faster in the pores and so filling time decreases while the filling rate increases [26]. It was also found that the modified ITO prepared at -0.9 V deposition potential yielded the smallest  $\Delta E_p$  compared to the ZnO modified ITO prepared at -1.0 V and -1.1 V, hence having a more favorable and stable electrochemical behavior. Since  $\Delta E_p$  is the function of electron transfer rate, hence the lower the  $\Delta E_p$ , the greater the electron transfer rate. A small  $\Delta E_p$  indicates that the electrode is kinetically favorable and hence minimizing background current [27]. We chose -0.9 V as the optimum potential in the electrodeposition procedure for the next step of the experiment.

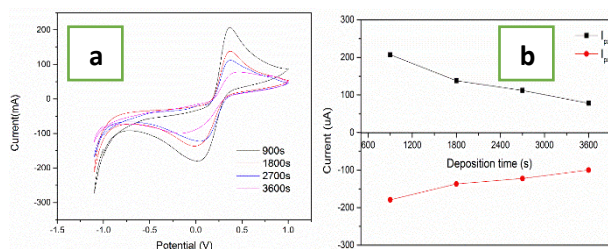
### 3.2.3 Effect of Deposition Time

Fig. 6 depicts the surface morphology of ZnO films prepared at various time ranging from 900 s to 3600 s with a constant bath temperature of 60 °C at -0.9 V. The SEM images indicate that the surface of the film appears to be denser at longer deposition time consisting of large and flat hexagonal grains with different orientations to the substrate



**Fig. 6** FESEM images of the ZnO nanorods (a) 900 s (b) 1800 s and (c) 2700 s (d) 3600.

At 900 s, the surface coverage is small, and increases with the deposition time. Apparent aggregates of small hexagonal grains could be observed upon deposition at higher deposition time. As the reaction time persisted to 3600, the compactness of the ZnO deposited is the highest with hexagonal rods covering the substrate



**Fig. 7** (a) Cyclic voltammogram of  $(\text{FeCN}_6)^{3-}$  at ZnO modified electrode prepared at various deposition time (900 s, 1800 s, 2700 s, and 3600 s) (b) Plot of anodic and cathodic peak currents behavior of ZnO modified ITO obtained at various deposition time

The electrochemical characterization of the ZnO modified ITO electrode prepared at various deposition potential time ranging from 900 s to 1800 s were carried out in the presence of  $K_3[Fe(CN)_6]$  ion in 0.1 M PBS electrolyte in order to evaluate the electrochemical behaviour. Fig. 7(a) depicts the voltammogram of 1.0 mM of potassium ferricyanide ( $K_3[Fe(CN)_6]$ ) in 0.1 M PBS electrolyte at the ZnO modified ITO electrodes. The improvement in current signal enhancement for anodic and cathodic peak corresponds to the decrease of deposition time during the electrodeposition process at -0.9 V at 60 °C bath temperature. The voltammogram produced appears quasi reversible at the ZnO modified electrode prepared at different deposition time. ZnO modified ITO prepared at 900 s deposition time yielded the highest anodic and cathodic peak current at 207.15  $\mu$ A and -197.11  $\mu$ A at the anodic and cathodic peaks respectively. At 1800 s, the redox peaks diminished to 138.18  $\mu$ A and -136.81  $\mu$ A. At 2700 s the redox peaks current continue to drop to 112.03  $\mu$ A and -122.44  $\mu$ A. While at 3600 s the redox peak current were 77.82  $\mu$ A and -99.98  $\mu$ A at the anodic and cathodic peaks respectively. The oxidation peak for the ZnO modified electrode prepared at 900 s enhanced with a factor of 2.66 when comparing to the ZnO modified electrode prepared at 3600 s. The peak currents obtained are well defined with  $I_{pa}/I_{pc} = 1.157$  and a peak separation of 0.32 V based on Fig. 7(b). The underlying reason behind the decrease of peak current with the increase of can be explained from the increase in film thickness as it increases with the deposition time. The thicker ZnO layers can efficiently work as hole-blocking layers to prevent the current leakage [28].

#### 4. Conclusion

The study on the different parameters during ZnO electrodeposition was studied. Among them was the effect of deposition potential, deposition time and deposition temperature. It was found that at higher deposition temperature will decrease the electrochemical behaviour of the ZnO modified electrode of  $K_3[Fe(CN)_6]$  in 0.1 M PBS electrolyte. The same behavior can be observed with the increase in deposition potential and deposition time. The morphology of the electrodeposited film showed that hexagonal pillar ZnO were fairly distributed with increasing surface area coverage for increasing temperature, deposition potential and deposition time. The three parameters studied showed to be important selection to obtain the desired morphology and electrochemical behaviour of the modified electrode. This finding is paramount to find a ZnO based sensor with increased sensitivity.

#### Acknowledgement

We would like to thank the School of Graduate Studies, Universiti Putra Malaysia for the financial support from the Graduate Research Fund (GRF) and Ministry of Higher Education for the MyBrain15 scholarship awarded to Alvin Lim Teik Zheng.

#### References

[1] J.J. Gooding, M.H.L. Lai, Y.G. Ian, Nanostructured electrodes with unique properties for biological and other applications, *Chem. Modif. Electrode* 11 (2009) 1–56.  
 [2] R. Montes, J. Bartrolí, M. Baeza, F. Céspedes, Improvement of the detection limit for biosensors: Advances on the optimization of biocomposite composition, *Microchem. J.* 119 (2015) 66–74.  
 [3] A.H. Moharram, S.A. Mansour, M.A. Hussein, M. Rashad, Direct precipitation and characterization of ZnO nanoparticles, *J. Nanomater.* 2014 (2014) 1–5.

[4] X. Wang, S. Yang, X. Yang, D. Liu, Y. Zhang, J. Wang, et al., ZnO thin film grown on silicon by metal-organic chemical vapor deposition, *J. Cryst. Growth.* 243 (2002) 13–18.  
 [5] B. Baruwati, D.K. Kumar, S.V. Manorama, Hydrothermal synthesis of highly crystalline ZnO nanoparticles: A competitive sensor for LPG and EtOH, *Sensors Actuat. B Chem.* 119 (2006) 676–682.  
 [6] G. Jiangfeng, D. Zhaoxing, D. Qingping, X. Yuan, Z. Weihua, Controlled synthesis of ZnO nanostructures by electrodeposition method, *J. Nanomater.* 2010 (2010) 1–6.  
 [7] N. Orhan, M.C. Baykul, Solid-State electronics characterization of size-controlled ZnO nanorods produced by electrochemical deposition technique, *Solid State Electron.* 78 (2012) 147–150.  
 [8] S. Peulon, D. Lincot, Cathodic electrodeposition from aqueous solution of dense or open-structured zinc oxide films, *Adv. Mater.* 8 (1996) 166–170.  
 [9] G. Bhanjana, N. Dilbaghi, R. Kumar, S. Kumar, Zinc oxide quantum dots as efficient electron mediator for ultrasensitive and selective electrochemical sensing of mercury, *Electrochim. Acta.* 178 (2015) 361–367.  
 [10] K. Shavanova, Y. Bakakina, I. Burkova, I. Shteplyuk, R. Viter, A. Ubelis, et al., Application of 2D non-graphene materials and 2D oxide nanostructures for biosensing technology, *Sensors (Switzerland)* 16 (2016) 1–23.  
 [11] M. Marie, S. Mandal, O. Manasreh, An electrochemical glucose sensor based on zinc oxide nanorods, *Nanorod. Nanosens.* 15 (2015) 18714–18723.  
 [12] A.S. Kazemi, R. Afzalzadeh, M. Abadyan, ZnO Nanoparticles as ethanol gas sensors and the effective parameters on their performance, *J. Mater. Sci. Technol.* 29 (2013) 393–400.  
 [13] S. Bhatia, N. Verma, R.K. Bedi, Ethanol gas sensor based upon ZnO nanoparticles prepared by different techniques, *Results Phys.* 7 (2017) 801–806.  
 [14] M.N. Cardoza-Contreras, J.M. Romo-Herrera, L.A. Ríos, R. García-Gutiérrez, T.A. Zepeda, O.E. Contreras, Single ZnO nanowire-based gas sensors to detect low concentrations of hydrogen, *Sensors (Switzerland)* 15 (2015) 30539–30544.  
 [15] L. Cui, G.G. Wang, H.Y. Zhang, R. Sun, X.P. Kuang, J.C. Han, Effect of film thickness and annealing temperature on the structural and optical properties of ZnO thin films deposited on sapphire (0001) substrates by sol-gel, *Ceram. Int.* 39 (2013) 3261–3268.  
 [16] S. Marouf, A. Beniaiche, H. Guessas, A. Azizi, Morphological, structural and optical properties of ZnO thin films deposited by dip coating method, *Mater. Res.* 20 (2017) 88–95.  
 [17] B.N. Illy, A.C. Cruickshank, S. Schumann, D. Campo, T.S. Jones, S. Heutz, et al., Electrodeposition of ZnO layers for photovoltaic applications: controlling film thickness and orientation, *J. Mater. Chem.* 21 (2011) 12949–12957.  
 [18] S. Hori, T. Suzuki, T. Suzuki, S. Miura, S. Nonomura, Effects of deposition temperature on the electrochemical deposition of zinc oxide thin films from a chloride solution, *Mater. Trans.* 55 (2014) 728–734.  
 [19] A. Azizi, M.R. Khelladi, L. Mentar, V. Subramaniam, A study on electrodeposited of zinc oxide nanostructures, *Akad. Platf.* (2013) 559–567.  
 [20] B.R. Scharifker, J. Mostany, Electrochemical nucleation and growth, in: *Encyclopedia Electrochemistry*, Wiley-VCH Verlag GmbH & Co. KGaA, Germany, 2007.  
 [21] M.R. Khelladi, L. Mentar, M. Boubatra, A. Azizi, Study of nucleation and growth process of electrochemically synthesized ZnO nanostructures, *Mater. Lett.* 67 (2012) 331–333.  
 [22] D. Pradhan, K.T. Leung, Vertical growth of two-dimensional zinc oxide nanostructures on ITO-coated glass, *J. Phys. Chem. C.* (2008) 1357–1364.  
 [23] Z.N. Nkunu, G.N. Kamau, J.G. Kithure, C.N. Muya, Electrochemical studies of potassium ferricyanide in acetonitrile-water media (1:1) using cyclic voltammetry method, *Int. J. Sci. Res. Innov. Technol.* 4 (2017) 52–58.  
 [24] J. Li, Z. Liu, E. Lei, Z. Zhu, Effects of potential and temperature on the electrodeposited porous zinc oxide films, *J. Wuhan Univ. Technol. Sci. Ed.* 26 (2011) 47–51.  
 [25] A.C. Cruickshank, S.E.R. Tay, B.N. Illy, R. Da Campo, S. Schumann, T.S. Jones, et al., Electrodeposition of ZnO nanostructures on molecular thin films, *Chem. Mater.* 23 (2011) 3863–3870.  
 [26] A. Prună, D. Pullini, D.B. Mataix, Influence of Deposition potential on structure of ZnO nanowires synthesized in track-etched membranes, *J. Electrochem. Soc.* 159 (2012) 92–98.  
 [27] M.E.G. Lyons, G.P. Keeley, The redox behaviour of randomly dispersed single walled carbon nanotubes both in the absence and in the presence of adsorbed glucose oxidase, *Sensors* 6 (2006) 1791–1826.  
 [28] Z. Liang, Q. Zhang, L. Jiang, G. Cao, ZnO cathode buffer layers for inverted polymer solar cells, *Energy Environ. Sci.* 8 (2015) 3442–3476.